

1 **On the spectral hardening at  $\sim > 300$  keV in solar flares**

2 G. Li<sup>1,\*</sup>, X. Kong<sup>2,1</sup>, G. Zank<sup>1</sup>, Y. Chen<sup>2</sup>

3 <sup>1</sup> Department of Physics and CSPAR, University of Alabama in Huntsville, Huntsville, AL  
4 35899, USA

5 <sup>2</sup> Institute of Space Sciences and School of Space Sciences and Physics, Shandong  
6 University, Weihai, China, 264209

7 \* gang.li@uah.edu

8 Received \_\_\_\_\_; accepted \_\_\_\_\_

**ABSTRACT**

It has been noted for a long time that the spectra of observed continuum emissions in many solar flares are consistent with double power laws with a hardening at energies  $\sim > 300$  keV. It is now largely believed that at least in electron-dominated events the hardening in photon spectrum reflects an intrinsic hardening in the source electron spectrum. In this paper, we point out that a power law spectrum of electron with a hardening at high energies can be explained by diffusive shock acceleration of electrons at a termination shock with a finite width. Our suggestion is based on an early analytical work by Drury et al., where the steady state transport equation at a shock with a tanh profile was solved for a  $p$ -independent diffusion coefficient. Numerical simulations with a  $p$ -dependent diffusion coefficient show hardenings in the accelerated electron spectrum which are comparable with observations. One necessary condition for our proposed scenario to work is that high energy electrons resonate with the inertial range of the MHD turbulence and low energy electrons resonate with the dissipation range of the MHD turbulence at the acceleration site, and the spectrum of the dissipation range  $\sim k^{-2.7}$ . A  $\sim k^{-2.7}$  dissipation range spectrum is consistent with recent solar wind observations.

*Subject headings:* Sun: flares — Sun: particle emission — Sun: X-rays, gamma rays  
— acceleration of particles

## 1. Introduction

13

14 Our Sun is an efficient particle accelerator. Ions with energy up to  $\sim GeV$ /nucleon are  
15 detected in-situ during large Solar Energetic Particle (SEP) events where both large flares  
16 and fast CMEs often occur together. At flares, electron Bremsstrahlung is believed to be  
17 the main source of the continuum radiation (e. g. Ramaty et al. (1975); Vestrand (1988)).

18 Continuum emissions provide invaluable information that constrains the underlying  
19 acceleration mechanism. These constraints include the energy budget, the total number  
20 of electrons, the acceleration time scales, etc. See reviews by Miller et al. (1997) and  
21 Zharkova et al. (2011) for a detail discussion on various acceleration mechanisms and the  
22 implications of these constraints on them.

23 One observational constraint that received less attention, even though has been noted  
24 for a long time, is the hardening of the continuum spectrum at high energies (often  $\sim > 300$   
25 keV). In 1975, Suri et al. (1975) examined the X-ray and gamma-ray flux in the August  
26 4, 1972 event and concluded that the X and gamma-ray flux was produced by a single  
27 population of electrons with a break in its spectrum, instead of two separate populations  
28 acting independently. Later, Yoshimori et al. (1985) , using Hinotori spacecraft, examined  
29 the hard X-ray (HXR) spectrum in a broad energy range (20 keV - 7 MeV) for four flares  
30 that showed significant hardening at energies above  $\sim 400$  keV. They confirmed the earlier  
31 suggestion of Suri et al. (1975) that the hardening in the continuum reflects an underlying  
32 hardening in the source electron spectrum. Spectral hardening also occur in events where  
33 there are clear signatures of gamma-ray lines. The most recent report of such an event is  
34 from the Fermi observation (see Ackermann et al. (2012)) where spectral hardening was  
35 found at above several hundred keV.

36 Note that hardening in the source electron spectrum is not the only cause for  
37 a hardening in the photon spectrum. Various processes, such as electron-electron

38 Bremsstrahlung, proton Bremsstrahlung, positronium annihilation continuum and inverse  
39 Compton emissions (see Vestrand (1988)), may all lead to some hardening of a continuum  
40 emission from a straight power law (without hardening) source electron spectrum. However,  
41 for parameters appropriate to a solar flare site, the contributions of these processes  
42 are relatively small and the resulting hardening of the spectral index is perhaps  $\sim 0.5$   
43 (Kontar et al. 2007). Therefore these processes can not explain events where the change  
44 of spectral indices are as high as 2. Park et al. (1997) studied photon spectral hardening  
45 around 1 MeV for four flares. In their scenario, the emission is a simple sum of the thin  
46 target emission from the trapped electrons at the acceleration site near the loop top and the  
47 thick target emission from the escaping electrons precipitating on the solar surface. With  
48 the assumption that electrons having smaller energies have shorter escape times, and noted  
49 that the energy dependence of the Bremsstrahlung cross section differs in the nonrelativistic  
50 and the relativistic regimes, Park et al. (1997) were able to account for the observed spectral  
51 hardening. Note in the scenario of Park et al. (1997), the energy dependence of the escaping  
52 time decides the hardening, and the accelerated electron spectrum in the accelerated region  
53 does not (need to) have a spectral hardening. In-situ observations by Moses et al. (1989),  
54 however, showed that electron spectral hardening is rather common in short duration events.  
55 Assuming these in-situ electrons are the source electrons escaping from the acceleration site  
56 through interchange reconnection, then Moses et al. (1989)’s results also suggest that the  
57 accelerated electron population has a hardening at high energies.

58 High energy electrons also lead to microwave emissions through gyro-synchrotron  
59 radiation (see e.g. the recent review by White et al. (2011) for a detailed discussion of the  
60 relationship between solar radio and HXR emissions). In an early study, using BATSE  
61 (HXRs) and Owens Valley Radio Observatory (microwaves), Silva et al. (2000) examined  
62 27 solar flares with multiple peaks (a total of 57) which were observed at both HXR and  
63 microwave wavelengths. Fitting the HXR spectra by a single power law and the microwave

64 spectra as gyrosynchrotron emissions, Silva et al. (2000) found that in 75% of the bursts,  
65 the inferred spectral indices of the electron energy distribution of the microwave-emitting  
66 electrons were harder (by 0.5 to 2.0) than those of the lower energy HXR emitting electrons.  
67 Silva et al. (2000) concluded that there exists a breakup in the energy spectra of the source  
68 electrons at around  $\sim 300$  keV, in agreement with previous observations of HXR-alone  
69 spectra of giant flares.

70 Note, however, in most events the HXRs are emanated from the footpoints of flare  
71 loops and microwaves are emanated from the tops of flare loops. Furthermore, there is also  
72 a delay between the peak of the microwave emission and the HXR emission. So there are  
73 transport effects between electrons generating microwave emissions and those generating  
74 HXRs White et al. (2011). Both the harder HXR spectrum at the footpoints and the delays  
75 of the microwave emission could be caused by magnetic trapping of higher energy electrons  
76 near the looptop and the precipitation of lower energy electron to the footpoints, as first  
77 suggested by Melrose and Brown (1976). In a recent study by Kawate et al. (2012), HXR  
78 and microwave emissions from 10 flares were analyzed. Although the emissions were at  
79 different locations and the spectral indices for microwave emissions are harder than those of  
80 the HXRs, by assuming a spectrum for the accelerated electrons that is consistent with the  
81 HXR emissions (but extend to higher energies), Kawate et al. (2012) were able to produce  
82 microwave spectra comparable to the observations. The authors concluded that it is a  
83 single electron population that is responsible for the HXRs and microwaves emissions and  
84 the hardening of the microwave emission is due to a more efficient trapping of electrons  
85 with higher energies. In another study, to minimize the effect of the trapping of high  
86 energy electrons on the resulting spectra of looptop microwave emissions, Asai et al. (2013)  
87 examined both the HXR and microwave spectra prior to the peak emission in 12 flares.  
88 They still find a significant hardening of the source electrons for the microwave emissions.  
89 These authors suggest that there is an intrinsic spectral hardening for the source electron

90 spectrum around several hundreds of keV and the microwave gyrosynchrotron emission is  
91 due to electrons at higher energies (in the harder part of the spectrum).

92 In this work, we do not consider microwave emissions and focus on HXR alone.  
93 Vestrand et al. (1999) identified 258 flare events using SMM observations. Among these,  
94 many are electron-dominated events with no clear signature of gamma-ray emissions  
95 (Rieger & Marschhauser 1990; Marschhauser et al. 1994). In these events, the contribution  
96 of nuclear gamma ray lines is minimal and the continuum is mainly due to Bremsstrahlung  
97 of the energetic electrons. The spectral hardening can be clearly seen in many of those  
98 electron-dominate events. A careful examination of these events based on the mechanism  
99 proposed here will be reported elsewhere (Kong et al. to be submitted).

100 A hardening in the source electron spectra is hard to explain for any acceleration  
101 mechanism. In this paper, we propose a scenario which is based on diffusive shock  
102 acceleration (DSA) to explain the observed spectral hardening.

103 Electron acceleration at a termination shock (TS) in solar flares is not a new idea.  
104 Tsuneta & Naito (1998) were the first to consider electron acceleration via DSA at a flare  
105 TS. Tsuneta & Naito (1998) pointed out that slow shocks bounding the reconnection  
106 X-point can heat the plasma up to perhaps 10-20 MK, providing abundant seed population  
107 which are accelerated to 1 MeV in 0.3 to 0.6 seconds at the TS.

108 Noting that the standing TS is of quasi-perpendicular in nature, Mann et al. (2009)  
109 considered shock drift acceleration (SDA) at a standing TS. In the work of Mann et al.  
110 (2009), most energy gain of electrons is through a single reflection at the shock front.  
111 Therefore to accelerate electrons to high energies, a stringent requirement of  $\theta_{BN}$  (e.g.  
112  $\theta_{BN} > 88^\circ$ ) is needed. However, while the TS on large scale is of quasi-perpendicular,  
113 small scale structures (such as ripples) exist on the shock front. Indeed, the plasma in the  
114 reconnection region is unlikely to be homogeneous, so the resulting TS is unlikely to be

115 planar. Recently, Guo & Giacalone (2012) have examined electron acceleration at a flare  
116 TS using a hybrid code. In the simulation of Guo & Giacalone (2012), many small scale  
117 ripples were identified along the shock surface. The existence of these ripples suggests  
118 that assuming a shock with a  $\theta_{BN} > 88^\circ$  across the shock surface may be unrealistic.  
119 Furthermore, the existence of these small scale structures implies that one single field line  
120 can intersect the shock surface multiple times. Consequently, the acceleration process will  
121 be of diffusive in nature. In this work, we follow Tsuneta & Naito (1998) and assume  
122 the electron acceleration at a flare shock can be described by the DSA mechanism. Note  
123 that the existence of a TS in a flare site is not trivial. Observational evidence of flare  
124 TS has been reported by Warmuth et al. (2009), who used dynamic radio spectrum from  
125 the Trensdorf radiospectrograph to show that there was a type-II radio bursts from a  
126 standing TS at  $\sim 300$  MHz during the impulsive phase of the X1.7 flare of 2001 March  
127 29. Besides the existence of a TS, the area of the TS shock has also to be large enough  
128 ( $\sim 10^{20}$  cm<sup>2</sup> in large flares ) to account for the observed flux of HXRs generated by high  
129 energy electrons. By assuming a 50% contour of the NRH source at 327 MHz (see Figure 2  
130 of (Warmuth et al. 2009) ) being a proxy for the shock, Warmuth et al. (2009) estimated a  
131 shock area of  $\sim 1.3 \times 10^{20}$  cm<sup>2</sup> in the 2001 March 29 X1.7 flare. We do note that these areas  
132 are much larger than the areas of HXR sources and are more comparable to active region  
133 sizes. Whether or not the size of the TS can be this large remains to be examined. Using  
134 the same technique, Warmuth et al. (2009) nevertheless obtained similar areas for other  
135 events where TS were observed. Of course, for smaller flares (like M flares), the area of the  
136 active region is smaller and we expect the area of the shock is also smaller.

137 Besides shock acceleration, models based on stochastic (aka 2nd-order Fermi)  
138 acceleration exist. For example, Miller et al. (1996, 1997) assumed the presence of some  
139 large scale turbulence at the flare site and considered the coupled system of the wave  
140 cascading and particle acceleration. Miller et al. (1996, 1997) showed that various modes

141 of waves (Alfvénic and fast mode waves), as they cascade to small scales, can efficiently  
 142 accelerate both ions and electrons. Similar processes have also been studied by, for example,  
 143 Petrosian et al. (1994); Park et al. (1997). Unlike Miller et al. (1996, 1997), Petrosian et al.  
 144 (1994); Park et al. (1997) did not address the cascading of the turbulence and assumed the  
 145 wave spectra is given.

146 In this work, we do not consider stochastic acceleration. However, as in Petrosian et al.  
 147 (1994); Miller et al. (1996, 1997); Park et al. (1997), we assume the diffusion coefficient  $\kappa$  is  
 148 decided by the underlying turbulence power at a flare site.

## 149 2. Diffusive shock acceleration of electrons at a finite-width termination shock

At a piecewise shock, the standard steady state DSA predicts a power law spectrum  $\sim p^{-\alpha}$  for energetic particles. The power law spectral index  $\alpha$  is given by  $3s/(s-1)$ , where  $s = u_1/u_2$  is the compression ratio,  $u_1$  and  $u_2$  the upstream and downstream flow speed in the shock frame. In the case of a shock having a finite width  $\sim L_{diff}$ , Drury et al. (1982) showed that the spectral index depends on the shock width. Assuming the background fluid speed is given by a tanh profile:

$$u(x) = \frac{u_1 + u_2}{2} - \frac{u_1 - u_2}{2} \tanh(x/L_{diff}) \quad (1)$$

then the spectral index  $\alpha$  becomes (Drury et al. 1982),

$$\alpha = \frac{3s}{s-1} \left( 1 + \frac{1}{\beta_s} \frac{1}{s-1} \right) \quad (2)$$

where  $\beta_s$  is a dimensionless parameter and is related to the diffusion coefficient  $\kappa$  through,

$$\kappa = \beta_s (u - u_1)(u - u_2) \frac{dx}{du} = \beta_s \frac{u_1 - u_2}{2} L_{diff}. \quad (3)$$

150 Although Drury et al. (1982) considered only the case of  $p$ -independent  $\kappa$  where analytical  
 151 solutions can be obtained, one can see from the above that for a  $\kappa$  increasing with  $p$  the



152 spectrum will harden at high energies. Because the factor of  $1/\beta_s$  in equation (2), the  
 153 spectral index quickly approaches the limit of  $3s/(s - 1)$  when  $\beta_s \geq 1$ . When  $\beta_s$  is small,  
 154 however, the second term in the bracket of equation (2) dominates and the spectrum can  
 155 be very soft.

156 Clearly the momentum dependence of the diffusion coefficient  $\kappa$  decides the shape of  
 157 the spectrum. At a flare site, the  $\kappa$  of energetic electrons is decided by the turbulence  
 158 level. At large scales, the turbulence is of Alfvénic and particle-wave cyclotron resonance  
 159 can accelerate ions to high energies via the stochastic acceleration process (e.g. Miller et al.  
 160 (1997)). For electrons, except at very high energies, however, they do not resonate with  
 161 Alfvén waves, therefore they interact with other waves, for example, fast mode and/or  
 162 whistler waves (Miller et al. 1996).

163 Note that Drury et al. (1982) did not consider the effect of the energetic electrons  
 164 on the shock. In a more refined and self-consistent analysis, the pressure of the energetic  
 165 electrons needs to be taken into account and it will affect the shock width. This is  
 166 similar to a modified shock structure caused by energetic cosmic rays as first examined by  
 167 Axford, Leer & McKenzie (1982). Such a discussion, however, exceeds the scope of this  
 168 work and we do not consider the back reaction of energetic electrons on the shock structure.

We assume the turbulence at a flare, as in the solar wind, is described by an inertial  
 range joining to a dissipation range and the power density  $I(k)$  is given by,

$$I(k) = I(k_0) \left( \left( \frac{k}{k_b} \right)^{-\epsilon_i} H(k_b - k) + \left( \frac{k}{k_b} \right)^{-\epsilon_d} H(k - k_b) \right), \quad (4)$$

where  $\epsilon_i$  and  $\epsilon_d$  are the spectral indices in the inertial range and dissipation range,  
 respectively. We assume  $\epsilon_d = 2.7$  (see below) and consider three cases for  $\epsilon_i$ :  $5/3$ ,  $1.5$  and  
 $1.0$ . The case of  $\epsilon_i = 5/3$  corresponds to a Kolmogorov cascading; the case of  $\epsilon_i = 1.5$   
 corresponds to a Iroshnikov-Kraichnan (IK) cascading, and the case of  $\epsilon_i = 1.0$  corresponds  
 to a Bohm-like diffusion (see below). At very small  $k$ , the energy containing range sets in

and  $I(k)$  bent over. The normalization of  $I(k)$  is given by,

$$\int_{-\infty}^{+\infty} I(k) = \langle \delta B^2 \rangle . \quad (5)$$

For a wide range of electron energy, the resonating wavenumber  $k$  is in the dissipation range. In the solar wind, one finds a spectrum  $\sim k^{-2.7}$  to  $\sim k^{-3.0}$  in the dissipation range (Leamon et al. 1998, 1999; Chen et al. 2010; Howes et al. 2011; Alexandrova et al. 2012). Unlike the inertial range, the nature of the turbulence in the dissipation range is still under debate. Two possible scenarios include Landau damping of kinetic Alfvén waves e.g. (Leamon et al. 1999, 2000; Boldyrev and Perez 2012) , or whistler waves e.g. (Stawicki et al. 2001; Krishan & Mahajan 2004; Galtier 2006) . For KAWs,  $k_{\perp} \gg k_{\parallel}$ , electron-wave interaction is through the Landau resonance and KAWs can effectively heat electrons. Whistler waves have  $\omega_p < \omega < \Omega$  and electrons can interact with whistler waves through the cyclotron resonance. The resonance condition is,

$$\omega - k_{\parallel}v_{\parallel} = n\Omega \quad (6)$$

where  $\Omega = eB/(\gamma m_e)$  is the electron cyclotron frequency and  $\gamma$  is the Lorentz factor. For low frequency waves  $\omega < \Omega$ , the resonance condition (on taking  $n = 1$ ) yields

$$\mu v = \Omega/|k_{\parallel}| \quad (7)$$

where  $\mu$  is the pitch angle of the electron. Note from equation (6), one can see that when the energy of electron is high enough, it can also resonate with Alfvén waves. In this work, we assume the dissipation range turbulence is whistler-wave-like and electrons can resonate with the wave through the cyclotron resonance. As done in Gordon et al. (1999); Rice et al. (2003); Li et al. (2005), we further simplify the resonance condition by replacing  $k = \Omega/\mu v$  with  $k = \Omega/v$ , which corresponds to an extreme resonance broadening. The pitch angle diffusion coefficient  $D_{\mu\mu}$ , from the Quasi-linear Theory (QLT) (Jokipii 1966) is,

$$D_{\mu\mu} = \frac{1 - \mu^2}{|\mu|v} \frac{\Omega^2}{B_0^2} I(k = \Omega/\mu v) \quad (8)$$

The diffusion coefficient  $\kappa$  is related to  $D_{\mu\mu}$  through,

$$\kappa = \frac{v^2}{8} \int_{-1}^{+1} \frac{(1 - \mu^2)^2}{D_{\mu\mu}} = \frac{v^3 B_0^2}{16\Omega^2 I(k = \Omega/v)} \quad (9)$$

We make no attempts to estimate the turbulence level at the reconnection site in this work. Instead, we are more interested in the energy dependence of  $\kappa$ . From equation (9), we have

$$\kappa = \kappa_0 \frac{(p/p_0)^{3-\epsilon_{i,d}}}{\gamma} \quad (10)$$

169 where subscripts  $i$  or  $d$  denote whether electrons resonate with the inertial or the dissipation  
 170 range of the turbulence. For electrons resonating with the dissipation range that have  
 171 a  $\epsilon_d \sim 2.7$ , equation (10) suggests that  $\kappa$  has a very shallow dependence on electron  
 172 momentum (energy). In comparison, for electrons resonating with the inertial range,  $\kappa$   
 173 increases quickly with particle momentum (energy). In Tsuneta & Naito (1998), the Bohm  
 174 diffusion approximation was used, in which case  $\kappa \sim vR_l$ , where  $R_l$  is electron's gyroradius.  
 175 This corresponds to an  $\epsilon_i = 1$ .

The fact that  $\kappa$  has a very shallow dependence on the electron's momentum in the dissipation range and a strong dependence in the inertial range is the key to understand the hardening of electron spectrum. In Figure 1 we plot  $\beta_s$  as defined in equation (3), where from equation (10), we have

$$\beta_s = \beta_0 \frac{(p/p_0)^{3-\epsilon_{i,d}}}{\gamma} \quad (11)$$

176 We set  $\beta_0 = 0.2$ . This value yields an electron spectral index at low energy to be  $\sim p^{-10}$ ,  
 177 comparable to flare observations.

178 Note, from equation (3),  $\beta_s$  also depends on the width of the shock. Simulations by  
 179 Scholer & Burgess (2006) suggested that the shock width is of the order of ion inertial  
 180 scale length  $\sim (c/\omega_{pi})$ . On the other hand, observations of the Earth's bow shock (at  
 181 quasi-perpendicular configurations) showed that its ramp width is somewhat smaller than

182  $\sim (c/\omega_{pi})$  (Scudder et al. 1986; Balikhin et al. 1995; Newbury et al. 1998). In particular,  
 183 Newbury et al. (1998) found considerable fine structures of the order of  $\sim (c/\omega_{pe})$ .  
 184 Zank et al. (2001) suggested that these fine structures will help to circumvent the injection  
 185 problem for Anomalous cosmic rays. In a very recent study, using Clusters observation,  
 186 Schwartz et al. (2011) showed that at the Earth’s bow shock half of the temperature  
 187 occurred in about  $\sim 7c/\omega_{pe}$  or  $\sim (1/7)c/\omega_{pi}$ . The total width of the shock in Schwartz et al.  
 188 (2011), which is close to  $L_{diff}$  in our work, however, is another factor of  $\sim 6$  (see their  
 189 figure (3)). Therefore, in this work, we assume the shock width is given by the ion inertial  
 190 length scale  $L_{diff} \sim c/\omega_{pi}$ .

191 The break point  $p_b$  in Figure 1 is  $p_b \sim \gamma m_e \Omega / k_b$  with  $k_b$  the wave number separating  
 192 the inertial range and the dissipation range. The scale at which the inertial range transits  
 193 into the dissipation range is still a much debated issue. It has been argued that it could  
 194 be the thermal proton Larmor radius  $\sim \frac{\sqrt{k_B T / m_p}}{\Omega_p}$  (Leamon et al. 1998, 1999) or the  
 195 ion inertial length  $\sim \frac{V_A}{\Omega_p}$  with  $\Omega_p$  the proton cyclotron frequency (Leamon et al. 2000;  
 196 Smith et al. 2001). Consider a typical flare site (Miller et al. 1996; Mann et al. 2009) with  
 197 a temperature of  $T \sim 5$  MK, a magnetic field of  $B \sim 200$  Gauss and a density of  $n_e \sim 10^9$   
 198  $\text{cm}^{-3}$ , we find an Alfvén speed  $V_A \sim 1.38 * 10^4 \text{ km sec}^{-1}$ , a thermal proton speed  $v_{th} \sim 200$   
 199  $\text{km sec}^{-1}$ , a proton gyrofrequency  $\Omega_p = 1.91 * 10^6 \text{ Hz}$ . Consequently, the thermal ion  
 200 Larmor radius is  $\sim 0.10 \text{ m}$  and the ion inertial length is  $\sim 7.2 \text{ m}$ . If  $k_b$  is the reciprocal of  
 201 the thermal ion Larmor radius, then  $p_b \sim 0.64 \text{ MeV}/c$  and the corresponding kinetic energy  
 202 is  $0.31 \text{ MeV}$ . This is in good agreement to the observed continuum emission break locations  
 203  $\sim 300 \text{ keV}$ . On the other hand, if  $k_b$  is the reciprocal of the ion inertial length, then  $p_b \sim 39$   
 204  $\text{MeV}/c$ , much too high for the proposed scenario. Therefore our proposed scenario favors  
 205 the the suggestion of Leamon et al. (1998, 1999) that the dissipation range sets in at the  
 206 thermal ion Larmor radius scale. Comparing to the width of the shock, which is the ion  
 207 inertial length scale  $7.2 \text{ m}$ , the gyro-radius of an electron  $R_l = \gamma v / \Omega_e$  is  $0.1 (0.4) \text{ m}$  for a

208 kinetic energy of 300 keV (2 MeV).

209 Using a momentum dependent  $\beta_s$  as in equation (11), we numerically solve the  
 210 steady-state transport equation. We set  $p_0$  to be 32 keV/c, which corresponds to an  
 211 injection energy of 1 keV. We use the same shock profile as Drury et al. (1982), given  
 212 by equation (1) and assume a compression ratio of 3.5 (thus a strong shock). Note that  
 213 the outflow plasma speed at a reconnection site is  $\sim V_A$ . Therefore for a shock with  
 214 a compression ratio of 3.5,  $u_1 - u_2$  in equation (3) is  $\sim 10^4$  km/s. We use  $\beta_0 = 0.2$ .  
 215 Tsuneta & Naito (1998) have used the Bohm approximation for  $\kappa$ . With the Bohm  
 216 approximation  $\kappa = \frac{1}{3}vR_l$  and the above values for a typical flare site, then a 300 keV  
 217 electron will have  $\beta_s = 0.2$  and a 2 MeV electron will have  $\beta_s = 1.0$ , suggesting our choice  
 218 of  $\beta_0 = 0.2$  is reasonable.

219 Figure 2 plots the steady state electron spectrum for three cases that have different  
 220 inertial range turbulence spectrum: i): Kolmogorov-like; ii): IK-like; and iii): Bohm  
 221 diffusion approximation. In each panel, the two dashed lines are power law fittings  
 222  $\sim (p/p_0)^{-\alpha}$ , with  $\alpha_1$  and  $\alpha_2$  the fitted spectral indices to the spectrum at the low and high  
 223 energies respectively, and  $p_m$  the fitted break momentum. We set  $p_b$  to be  $13p_0 \sim 0.416$   
 224 MeV/c in the simulation, which corresponds to a  $E_b$  of 0.15 MeV. Note that  $p_m$  is larger  
 225 than  $p_b = \gamma m_e \Omega / k_b$  by about a factor of  $\sim 2$ . Figure 2 is the most important result of this  
 226 paper. It shows that diffusive shock acceleration at a finite-width termination shock in solar  
 227 flares can naturally lead to a hardening of the accelerated electron spectrum.

### 228 3. Discussions and conclusions

229 Clearly, the hardening requires the following conditions to be met. First, the existence  
 230 of a termination shock at flare site with a finite shock width  $L_{diff} \sim c/\omega_{pi}$ . Second, the

231 diffusion coefficient  $\kappa$  needs to be close to a constant at low energies and increases with  
232 electron energy at high energies. Third, it is necessary that  $\kappa < \Delta UL_{diff}$  at energies below  
233 the break and  $\kappa > \Delta UL_{diff}$  at energies above the break.

234 For any given flare, none of these conditions are necessarily satisfied.

235 Consider the first condition. While it is hard to identify a termination shock at a flare  
236 observationally, there are indirect clues of such shocks. For example, type II radio bursts  
237 without frequency drift has been used by Warmuth et al. (2009) to infer the existence of  
238 flare termination shocks. Further observational evidence of flare termination shock, and in  
239 particular its size, are welcomed.

240 For the second condition: if electrons resonate with the dissipation range of the  
241 turbulence through cyclotron resonance and that the dissipation range has a power  
242 spectrum  $I(k) \sim k^{-2.7}$ , then we find  $\kappa$  is indeed close to a constant at low energies and  
243 increases with electron energy at high energies. While in-situ solar wind observations do  
244 suggest such a  $\sim k^{-2.7}$  dissipation range, direct confirmation of such a  $k$  dependence in the  
245 flare site is impossible.

246 To satisfy the third condition will put a strong constraint on the turbulence level at the  
247 flare, which can vary much from one to another. Consequently, the hardening does not occur  
248 in all flares. For example, if for a given flare,  $\beta_s \sim 1$  instead of  $\beta_s \sim 0.2$  at lower energies,  
249 then there will be no hardenings, even if both conditions 1 and 2 are satisfied. Because  
250 a larger  $\beta_s$  implies a larger  $\kappa$ , therefore a less efficient acceleration, so one implication of  
251 our proposed scenario is the following: Events where the continuum emission extend to  
252 very high energies (efficient acceleration) likely show hardenings and have softer spectra at  
253 lower energies, and events where the continuum emissions do not extend to high energies  
254 (inefficient acceleration) likely have harder spectra at low energies than those events that  
255 extend to higher energies.

256 Another consequence of our proposal is the correlation between the low energy photon  
257 spectral index  $\gamma_1$  and the break momentum  $p_m$ . Consider two nearly identical flares A and  
258 B except that flare A has a larger  $k_b$  (i.e. the inertial range in flare A extends to a smaller  
259 scale). Then  $\beta_s$  at  $p < p_m$  for flare A is smaller. Therefore,  $p_m$  and  $\alpha_1$  are anti-correlated.  
260 Observations do show such a anti-correlation and this is discussed in details in Kong et al.,  
261 (in preparation).

262 In summary, we offer an explanation for the observed continuum spectral hardening  
263 in solar flares that is based on DSA. To our knowledge, no previous works have addressed  
264 the hardening of emission spectrum explicitly. Further observational and theoretical studies  
265 along the proposed mechanism will be pursued in future works.

266 This work is supported in part by NSF grants ATM-0847719, AGS1135432, and NASA  
267 grants NNH07ZDA001N-HGI and NNX11AO64G at UAHuntsville and the 973 Program  
268 No. 2012CB825601 and NNSFC Grant Nos. 41274175 and 41028004 at SDUWH. XLK  
269 acknowledges financial support by the Shandong University Graduate Study Abroad Fund.

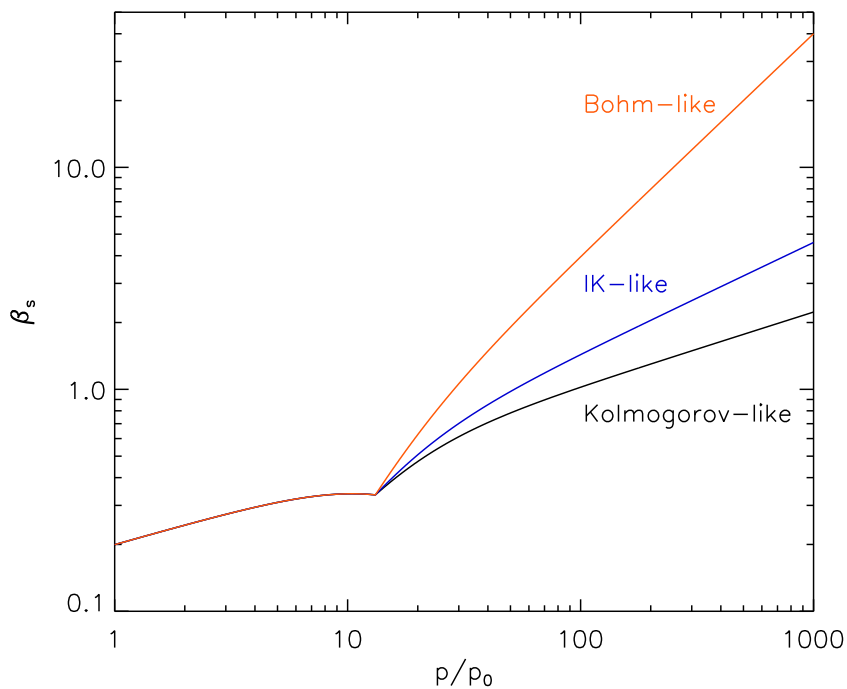


Fig. 1.—  $\beta_s$  as defined in equation (3). At low energies, electrons resonate with the dissipation range and  $\beta_s$  has a weak momentum dependence. Above  $p_b$ , electrons resonate with the inertial range and  $\beta_s$  quickly increases with momentum. Three cases for the inertial range are considered. These are, from top to bottom, Bohm-like, IK-like and Kolmogorov-like.



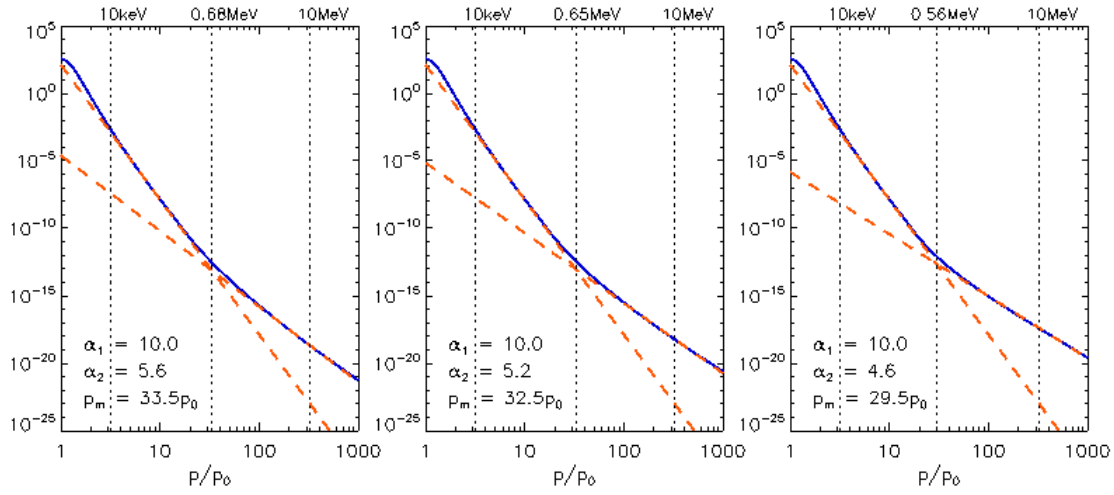


Fig. 2.— The electron spectrum for three cases: i: Kolmogorov-like inertial range; ii: IK-like inertial range; iii: Bohm diffusion Approximation.

**REFERENCES**

270

271 Alexandrova, O., Lacombe, C., Mangeney, A., Grappin, R., Maksimovi, M., 2012, ApJ, 760,  
272 121

273 Ackermann, M., Ajello, M., Allafort, A., et al. 2012, ApJ, 745, 144

274 Balikhin, M. A., Krasnosselskikh, V., & Gedalin, M. 1995, Adv. Space Res., 15, 247

275 Asai, A., Kiyohara, J., Takasaki, H., Narukage, N., Yokoyama, T., Masuda, S., Shimojo,  
276 M., and Nakajima, H., 2013, ApJ, 763, 87

277 Axford, W.I., Leer, E., and McKenzie, J.F., 1982, A& A, 111, 317

278 Boldyrev, S., and Perez, J. C., 2012, ApJL, 758, L44.

279 Chen, C. H. K., Horbury, T. S., Schekochihin, A. A., et al. 2010, Phys. Rev. Lett., 104,  
280 255002

281 Drury, L. O’C., Axford, W. I., Summers, D. 1982, MNRAS, 198, 883

282 Galtier, S. 2006, J. Plasmas Phys., 72, 721

283 Guo, F., & Giacalone, J. 2012, ApJ, 753, 28

284 Gordon, B. E., M. A. Lee, and E. Möbius, 1999, JGR, 104, 28263-28277.

285 Howes, G. G., Tenbarge, J. M., & Dorland, W. 2011, Phys. Plasmas, 18, 102305

286 Jokipii, J., 1966, ApJ, 146, 480.

287 Kawate, T., Nishizuka, N., Oi, A.; Ohyama, M., and Nakajima, H., 2012, ApJ, 747, 131

288 Kontar, E. P., Emslie, A. G., Massone, A. M., et al. 2007, ApJ, 670, 857

289 Krishan, V. & Mahajan, S. M. 2004, JGR, 109, A11105

- 290 Lee, M. A. 1983, JGR, 88, 6109
- 291 Li, G., Zank, G. P., Rice, W. K. M. 2005, JGR, 110,A06104
- 292 Lin, R. P., Dennis, B. R., Hurford, G. J., et al. 2002, Sol. Phys., 210, 3
- 293 Leamon, R. J., Smith, C. W., Ness, N. F., Matthaeus, W. H., Wong, H. K. 1998, JGR, 103,  
294 4775
- 295 Leamon, R. J., Smith, C. W., Ness, N. F., Wong, H. K. 1999, JGR, 104, 22331
- 296 Leamon, R. J., Matthaeus, W. H., Smith, C. W., et al. 2000, ApJ, 537, 1054
- 297 Mann, G., Warmuth, A., Aurass, H. 2009, A&A, 494, 669
- 298 Marschhauser, H., Rieger, E., Kanbach, G. 1994, AIP Conference Proceedings, 294, 171
- 299 Melrose, D. B., & Brown, J. C., 1976, MNRAS, 176, 15
- 300 Miller, J. A., Larosa, T. N., Moore, R. L., 1996, ApJ, 461, 445
- 301 Miller, J. A., Cargill, P. J., Emslie, A. G., et al., 1997, JGR, 102, 14631
- 302 Moses, D., Droge, W., Meyer, P., Evenson, P., 1989, ApJ, 346, 523.
- 303 Newbury, J. T., Russell, C. T., and Gedalin, M., 1998, J. Geophys. Res., 103, 29581
- 304 Park, B. T., Petrosian, V., Schwartz, R. A. 1997, ApJ, 489, 358
- 305 Petrosian, V., McTiernan, J. M., Marschhauser, H. 1994, ApJ, 434, 747
- 306 Ramaty, R., Kozlovsky, B., Lingenfelter, R. E. 1975, Space Sci. Rev., 18, 341
- 307 Rieger, E., & Marschhauser, H. 1990, in Proc. of the Third Max 91 Workshop, ed. R. M.  
308 Wingler & A. L. Kiplinger, 68

- 309 Rice, W. K. M., Zank, G. P., Li, G. 2003, JGR, 108, 1082
- 310 Scholer, M., & Burgess, D. 2006, Phys. Plasmas, 13, 062101
- 311 Schwartz, S. J., Henley, E., Mitchell, J., Krasnoselskikh, V. 2011, PRL, 107, 215002
- 312 Scudder, J. D., et al. 1986, J. Geophys. Res., 91, 1053
- 313 Silva, A. V. R., Wang, H., & Gary, D. E. 2000, ApJ, 545, 1116
- 314 Smith, C. W., Mullan, D. J., Ness, N. F., Skoug, R. M., Steinberg, J. 2001, JGR, 106, 18625
- 315 Stawicki, O., Gary, S. P., Li, H. 2001, JGR, 106, 8273
- 316 Suri, A. N., Chupp, E. L., Forrest, D. J., Reppin, C. 1975, Sol. Phys., 43, 415
- 317 Tsuneta, S. & Naito, T. 1998, ApJL, 495, L67
- 318 Vestrand, W. T. 1988, Sol. Phys., 118, 95
- 319 Vestrand, W. T., Share, G. H., Murphy, R. J., et al. 1999, ApJS, 120, 409
- 320 Warmuth, A., Mann, G., Aurass, H. 2009, A&A, 494, 677
- 321 White, S. M., Benz, A. O., Christe, S., Fárník, F., Kundu, M. R., Mann, G., Ning, Z.,  
322 Raulin, J.-P., Silva-Válio, A.V.R., Saint-Hilaire, P., Vilmer, N., Warmuth, A., 2011,  
323 Space Sci. Rev., 159, 225, doi: 10.1007/s11214-010-9708-1
- 324 Yoshimori, M., Watanabe, H., Nitta, N. 1985, JPSJ, 54, 4462
- 325 Zharkova, V. V., Arzner, K., Benz, A. O., et al. 2011, Space Sci. Rev., 159, 357
- 326 Zank, G. P., Rice, W. K. M., le Roux, J. A. and Matthaeus, W. H., 2001, ApJ, 556, 494